GROUND TRUTH LOCATIONS - A SYNERGY OF SEISMIC AND SYNTHETIC APERTURE RADAR INTERFEROMETRIC METHODS

C. K. Saikia,[1] R. Lohman,[2] G. Ichinose,[1] D. V. Helmberger,[2] M. Simons[2]and P. Rosen[3]

URS Group, [1] California Institute of Technology, [2] and Jet Propulsion Laboratory[3]

Sponsored by Defense Threat Reduction Agency

Contract Number DTRA01-00-C-0072

ABSTRACT

The primary objective of this study is to obtain reliable locations of moderate-sized ($4<M_w<6$) earthquakes in parts of Asia and the Middle East. The study is aimed at delivering a ground truth (GT) database consisting of locations, processed InSAR (Satellite Synthetic Aperture Radar Interferometry) phase and ground deformation maps for the general seismological community. We have developed combination of effective approaches to invert global travel-time phase data to obtain accurate locations. To this end, we have selected all events from the International Seismic Centre (ISC) bulletin that satisfy both GT10 and GT25 criteria and collected their phase data. From this entire event population, we selected a small set of events, estimated hypocentral depths by modeling the teleseismic depth phases and computed maps of surface deformation using software developed at USGS (United States Geological Survey) based on the equations of Okada (1992), which assumes an elastic half-space model. We are currently developing a code to include layered crustal model based on the frequency-wave number algorithm (Saikia, 1994). Surface deformation was computed to determine whether moderate-sized events that have larger depths (>10 km) would be resolvable in the processed InSAR interferograms, thus reducing the cost of radar data. We are currently processing the InSAR raw images obtained from EURIAMGE.

We present results obtained for one Southern Iran event (99/04/30, origin time:04h:20m:22.8s, 27.837^{o}N and 53.588^{o}E, 36km, M_w 4.9). We constructed two geocoded interferograms using images for track 20, frame 3051 (99/04/21-99/05/26) and for track 249, frame 3051 (99/04/02-99/06/11), respectively, by removing the topography (using a digital elevation model), filtering and unwrapping the phase. Note that these tracks include time period for at least three events occurring on the 28th and the 30th April and the 6th May of 1999 in Southern Iran. Of these, the third event is actually at more than a hundred miles from the track locations and is the largest (m_b~5.3). It is unlikely that the 05/06/99 event contributed to the interferograms because of its distance from the track. The remaining events are deep (h>30 km), and the 30th April event is larger. The geocoded interferogram show some earthquake deformation at 27.87^{o}N and 53.61^{o}E as a bulls eye of around two interferometric fringes. Both images have many elongated patterns throughout, but they correlate with the topography and have a much lower contribution to the interferograms than does the earthquake signal. The InSAR location is further away from the Harvard (27.74^{o}N, 52.96^{o}E), ISC and USGS (27.837^{o}N, 53.538^{o}E) locations and all have estimated depths that cannot lead to surface deformation to be discernable in the interferograms. This indicates that the contributing event is shallower (about 4 km) than the reported depths. To further ascertain the depth, we collected seismograms from all available stations. It was recorded at many stations, including those from temporary PASSCAL experiments. Of these, we compared seismograms from stations RAYN and ATD against a large shallow Southern Iran event (98/11/13, h=9 km, M_w=5.3). By analyzing seismograms from the April 30, 1999, and November 13, 1998, events we noted a high correlation in the different seismic wave groups, namely the P_{nl}, surface and high frequency Lg coda (>1Hz) waves. In addition to the amplitude, there is a good correlation in the travel times of these phases relative to their onset for the two events, indicating that the April 30 event (or the 28th event) is indeed shallow. We are now extending this analysis to other events in our study area and since many of the events are from the mountain regions, our analyses would also require high-resolution digital terrain elevation data.

OBJECTIVE

The goal of this ongoing study is to obtain reliable locations for moderate-sized ($4<M_w<6$) earthquakes in parts of Asia and the Middle East. This study will deliver a ground truth database consisting of locations, location errors, source parameters, associated waveform data, raw satellite synthetic aperture radar interferometry (InSAR) images, processed InSAR phase maps and ground deformation maps to the Center for Monitoring Research and the national laboratories. We will also provide these products to the general seismological community as well.

The basic goal of this study is improving of event locations that apparently satisfy the criterion of (GT)25 (e.g., Yang *et al*., 2000) for earthquakes which occurred in this study region to within an accuracy of (GT)10. To accomplish this goal, we developed a combination of approaches to invert global travel-time phase data to obtain accurate locations that prove effective (Saikia and Ichinose, 2001). This study also utilizes InSAR to locate shallow ($h<10$ km) and moderate-sized earthquakes for validating ground truth locations to within the level of 5 km location accuracy. We intend to determine the ground truth locations and fault parameters by modeling co seismic deformation observed from the processed InSAR images for comparison with prediction from seismology, which is an emerging technique. The final task is to combine the seismic and geodetic results to validate the GT locations. GT locations determined from InSAR will be used to develop station corrections for upper-mantle phase arrivals which in turn will be useful for relocating earthquakes within the magnitude range of ($4<M_w<5$) that are often recorded in this region by more than 30 stations within a distance of 20^o and with a maximum azimuthal gap of 90^o.

RESEARCH ACCOMPLISHED

The combination of InSAR and seismic data has a potential that remains relatively unexploited. Synthetic aperture radar interferometry developments have recently found applications to providing independent and ground-truth information based on ground surface deformation (e.g., Peltzer and Rosen, 1995; Feigl *et al.*, 1995; Massonnet, D., and K. L. Feigl, 1998; Lohman and Simons, 2000). Steck *et al*. (2000) used InSAR data to remove a location bias of 20 km for the relocation of the 1997 Tibetan mainshock (M_w 7.5). Correlating the co seismic fringe pattern derived from the InSAR data with hypocenter locations can be tricky because the centroid location may not necessarily coincide with the rupture initiation location for large earthquakes. Therefore, it is essential to concentrate on moderate-sized events (M_w~5) in order to reduce uncertainty in location due to the fault size. Earlier we investigated locations established through several InSAR analyses for earthquakes in various tectonic environments and compared with the locations determined by seismic methods using various strategic approaches (Saikia and Ichinose, 2001). In a continuing effort, we found that for earthquakes of Dec 12, 1992, Lander aftershock (M_w 5.4), June 29, 1992, Little Skull Mountain (M_w 5.6), Sept 07, 1999, Athens (M_w 5.9) and May 7, 1993, Eureka (M_w 6.1) it was possible to recover the seismic location within 10 km of the InSAR location. However, there is uncertainty in the location of the rupture initiation relative to the location proposed from the InSAR analysis for the two larger earthquakes. To this end, we have examined geodetic deformation and complexities in the teleseismic waveforms of a large earthquake (M_w 6.4) to check viability of a procedure that may be able to overcome this problem. In the following, we shall present preliminary results from this procedure.

To reduce the cost of radar data, we selected a small set of (GT)10 events spanning over the entire study region and depths down to 18 km. For each of these events, depths were estimated by modeling the pP and sP depth phases (Figure 1). We also computed the associated coseismic deformation using software developed at USGS (United States of Geological Survey) to ensure that the earthquakes are likely to cause some seismic deformation that will be recorded in the radar data. Next, we looked for tracks and frames for the radar data with small baseline (B). It is essential that B is small; otherwise there may be a lot of unwanted distortion in the phase interferogram, especially in a young tectonic regions (Rosen *et al*., 2000).

We studied a small event occurred in southern Iran on April 30, 1999 (see Table 1). Two geocoded interferograms were constructed using images for track 20, frame 3051 (99/04/21-99/05/26) and for track 249, frame 3051 (99/04/02-99/06/11), respectively, by removing the topography (using a digital elevation model, DEM), filtering and unwrapping the phase. Figure 2 shows the final phase interferogram where the earthquake can be seen to the upper right of the image at 27.89^oN and 53.62^oE as a bulls eye of around two interferometric fringes. The elongated pattern throughout these images correlates with the topography of the region of higher resolution. A further modeling of the InSAR amplitude indicated a shallow depth of 4 km for this event. The time between the first track

and last track included at least two other events occurring on the 28th April (18h:18m:18.8s, h=77km, m_b=4.5) and 6th May of 1999 (23h:00m:53.1s, 33km, m_b=5.9) in the vicinity of the 30th April event. The later event is too far away from the track locations to have contributed to the geodetic signal. Figure 3 shows a comparison of the uncorrected waveforms of events on the 28th and 30th recorded at a station RAYN in Saudi Arabia. The waveforms of the two events are remarkably similar indicating that the source mechanisms of the two events are similar. The peak amplitude is somewhat smaller for the 28th event. All reporting agencies indicated that these events are deep. Therefore, we compared its waveform with another event that occurred on 11/13/98 at the same location and depth of about 9 km (Figure 4). Figure 5 shows a comparison of waveforms between the events of 11/13/98 and 04/30/99 at RAYN at two frequency bands. The broadband displacement comparison shows strong Rayleigh waves on the 04/30/1999 event indicating that this event is shallower than event of 11/13/98. The longer duration of the high-frequency Lg waves for the 04/30/99 event also suggests that the event is more shallower than the 11/13/98 event.

Table 1 shows that the HRV location is the worst as it is about 65 km away from the InSAR location. We have also relocated this event using travel-time data and the constraints that depth is either free or fixed at 4 km. The location determined for the case when the depth is free, is about 3 km from the InSAR location. The location deteriorated when the depth was fixed by a mislocation of about 14 km. The USGS location remains within 10 km from the InSAR location. Finally, the event was fixed at the InSAR location and depth, and the best origin time was estimated (Table 1).

We finally present an indirect procedure which may be useful in recovering the hypocenter of a large magnitude earthquakes (M_w~6.5). The panel (b) of Figure 6 shows the slip model established for the Chi-Chi aftershock (Mw 6.4) by putting the hypocenter (shown by the star) in the upper left. We calculated theoretical InSAR data along the line of sight (panel c) using this slip model and hypocenter. Next, we reversed the problem and used this InSAR data shown in panel (c) and the teleseismic waveform as only the known data to invert for the hypocentral location. We divided the fault surface into many subfaults and varied the hypocenter location on the fault surface. For each hypocenter location, we estimated the misfit in teleseismic waveforms and the InSAR deformation (panel a). This misfit information was used to recover the original hypocenter location which is the star in panel (c). Our next step is to apply this approach to the some large earthquakes, such as the Eureka Valley earthquake of 05/17/1993 (Mw 6.0).

CONCLUSIONS AND RECOMMENDATION

Finding accurate ground-truth locations for earthquakes in areas where seismic network stations are sparse is often difficult because of the poor azimuthal station coverage. There may often be other logistical difficulties in accessing the local earthquake catalog. The InSAR analysis allows avoiding this shortcoming. The success with the 04/30/99 southern Iran earthquake demonstrates that seismic events can be located with a high level of accuracy through a synergy of InSAR and seismological methods that was illustrated by Saikia and Ichinose (2001). The only requirements are that the selected events are preferably shallow (say, h<10km) and have low magnitudes (M_w < 5.5). The low magnitude is preferred to minimize any uncertainty that may otherwise exist in case of the large magnitude earthquakes due to their large fault dimensions.

When the depth was known, the Iranian event was mislocated by 14.6 km relative to InSAR location, assumed as the ground truth location. On the other hand, when the depth was free, its location was off only by 3 km, suggesting that the earthquake location using the travel-time data alone is a highly non-linear process. Even the relative errors in the locations of the reference events can propagate systematic errors into the locations of other events. Therefore, ground truth locations based on the InSAR analysis are needed to evaluate the performance of any location scheme.

We have acquired SAR data of other earthquakes and the processing of data. In our continuing investigation to identify ground deformation in the InSAR images suggests that a high-resolution DEM model is essential for the SAR analysis to be successful in the area of our interest, especially in regions where ground surface topography is strong.

Large earthquakes often occur at shallow depth (h<15 km) and some leave extensive ground deformation. So far, they are not considered suitable for the purpose of ground truth locations because of the large extent of the fault dimensions and variability of the hypocenter location on the fault surface. Our on-going work on the Chi-Chi

aftershock and future plans to apply the approach to known large events for which geodetic signals have already been processed are aimed at avoiding these drawbacks.

ACKNOWLEDGEMENT

We thank our colleagues in EURIMAGE for making the radar data available to us urgently for this study.

REFERENCES

Feigl, K. L., A. Sergent, and D. Jack (1995). Estimation of an earthquake focal mechanism from a satellite radar interferogram: Application to the Dec 4, 1992 Landers aftershock, *Geophys. Res. Lett*., **22**, No. 9, 1037-1040.

Lohman, M., and M. Simons (2000). Interferometric synthetic aperture radar imagery of the June 29, 1992, Little Skull Mountain earthquake, *EOS Trans. AGU,* **90** *Fall Meeting Suppl*.

Massonnet, D., and K. L. Feigl (1998). Radar Interferometry and its application to changes in the Earth's surface, *Rev. Geophys.* **36**. No. 4, 441-500.

Peltzer, G., and P. A. Rosen (1995). Surface displacement of the 17 May, 1993 Eureka Valley, California, earthquake observed by SAR Interferometry, *Science*, **268**, 1333-1336.

Rosen, P. A., S. Hensley, I. R. Joughin, F.K.Li., S. N. Madsen, E. Rodriguez, R. M. Goldstein (2000). Synthetic Aperture Radar Interferometry, *Proceed. of the IEEE*, **88**, No. 3, March.

Saikia, C. K., and G. Ichinose, and C. Ji (2001). Seismic event location strategy and path calibration in and around Indian subcontinent, Proceed. 23rd Seism. Res. Rev., Worlwide Monitoring of Nuclear Explosions , October 2-5, 2001, Jackson Hole, Wyoming

Steck., L. K., A. A. Velasco, A. H. Cogbill, and H. J. Patton (2000). Improving regional seismic event location in China, *Pure and Applied Geophysics* (in press).

Yang, X., I. Bondár, and C. Romney (2000). PIDC ground-truth event (GT) database (revision 1). CMR Technical Report CMR-00/15.

Table 1. Location Parameters for April 30, 1999 Southern Iran Earthquake

Date d/m/y	**Origin Time Hr:mn:ss**	**Latitude (N deg)**	**Longitude (E deg)**	**H (km)**	**ΔR (km)**	**Agency**
04/30/99		27.870	53.610			INSAR
04/30/99	04:20:02.0	27.765	53.519	33.1	14.68	ISC (MOS)
04/30/99	04:20:22.5	27.837	53.538	35.0	7.0	USGS
04/30/99	04:19:59.6	27.748	53.553	4.0 (F)	14.6	URS
04/30/99	04:20:05.4	27.866	53.576	45.0	3.04	URS
04/30/99	04:20:12.5	27.74	52.960	44.9	65.65	HRV
04/30/99	**04:20:0.1**	**27.870 (F)**	**53.610 (F)**	**4.0 (F)**		**Seis+INSAR**

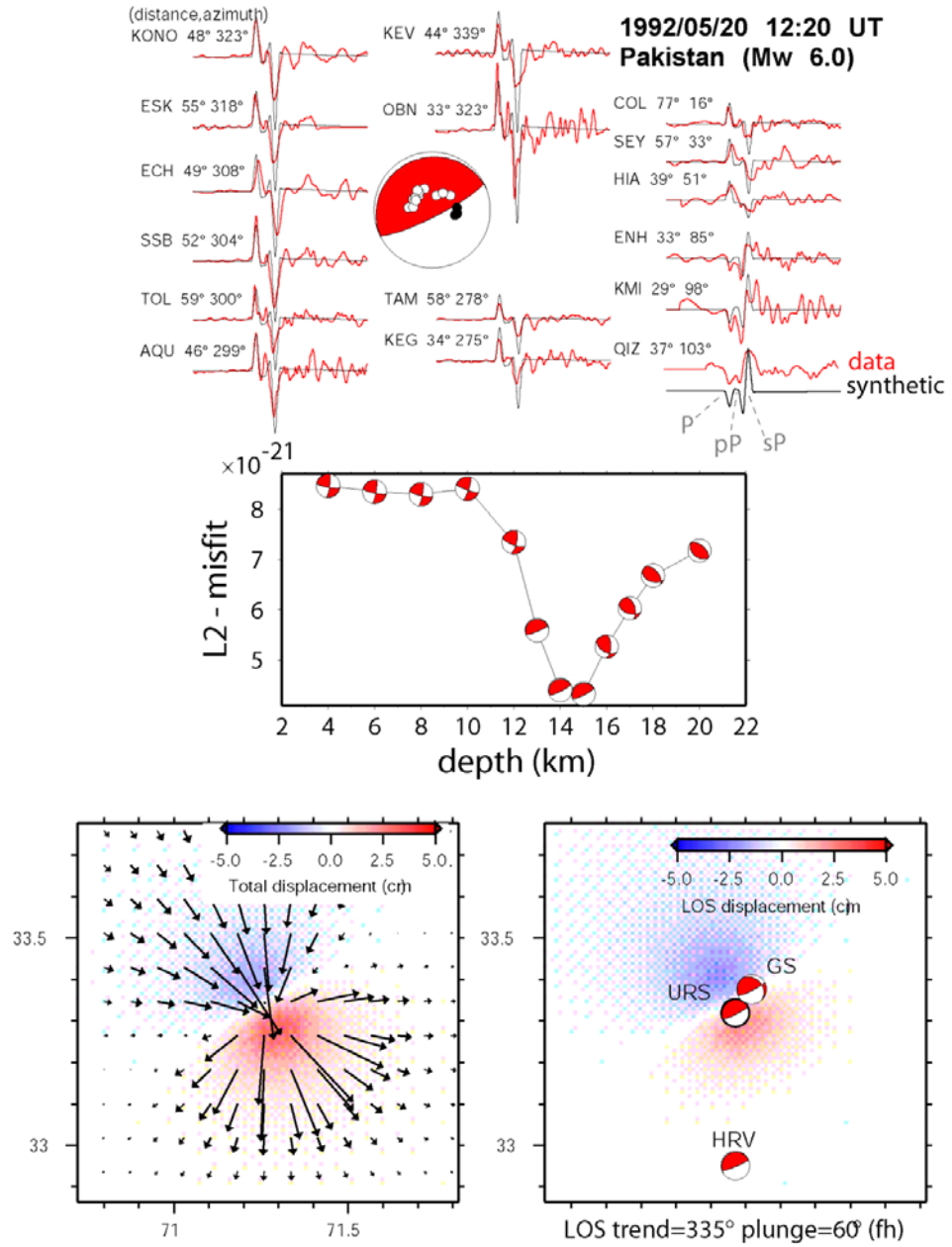

Figure 1. (top) Focal mechanism and (middle) hypocenter depth estimated from the inversion o teleseismic P-wave and depth phases. We determine these source parameters using a grid sear scheme. The resulting source parameters are then used to predict the coseismic deformation at the surface assuming an elastic halfspace. We do this for both nodal planes but since this event was relativly small and deep, there was no difference in deformation (not shown). See text for more details.

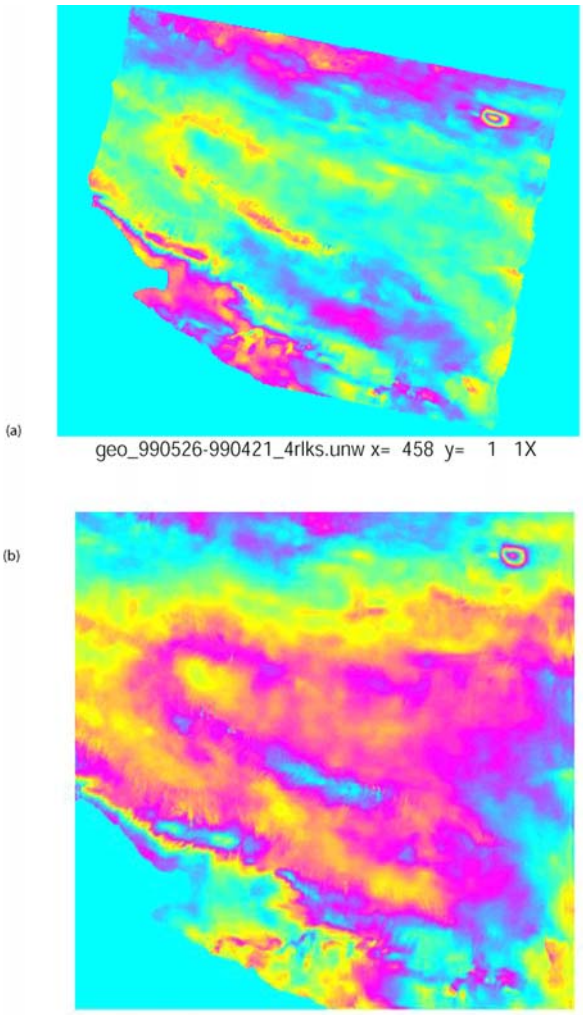

Figure 2. (a) Geocoded interferogram (99/04/21-99/05/26) for track 20 and frame 3051 (approximate geographic extents : 28.12N 52.70E; 27.94N 53.69E; (27.05E 53.48E and 27.23N, 52.50E. Topography is removed using DEM, filtered and unwrapped. The earthquake appears to the upper right of the image at 27.89N 53.61E as a bulleye of around 2 interferometric fringes. The other elongated patterns throughout the image correlate with topography and have much lower contribution to the interferogram than the earthquake signal. (b) This is a similar processing using low resolution topography removed

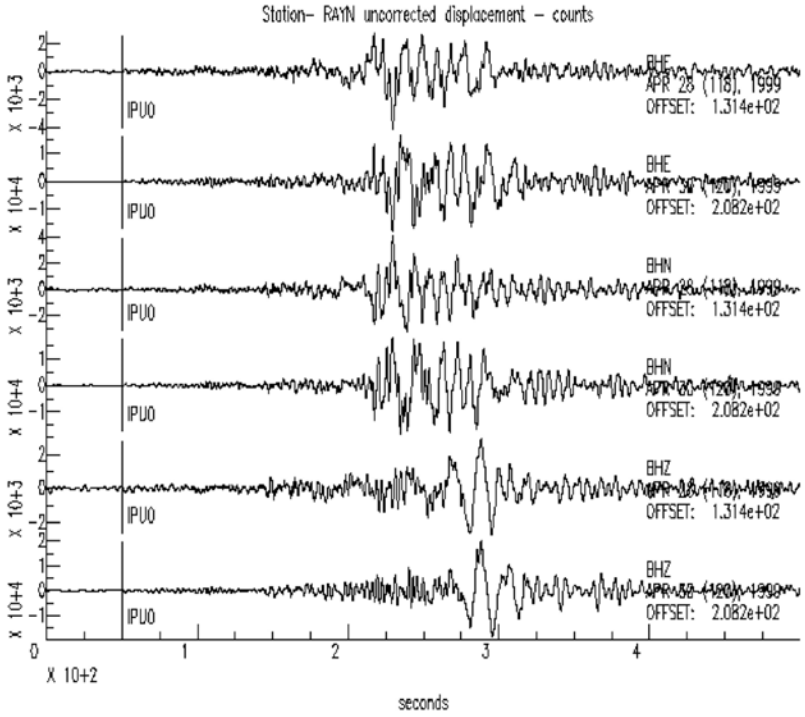

Figure 3. Comparison of broadband waveforms from two earthquakes in southern Iran. Note the similarities in waveforms. The events occurred only two days apart; the event of April 28 is smaller in magnitude. Although the both events may have contributed to the bulleye fringes in Figure 2, the event of the 30th April must have contibuted significantly.

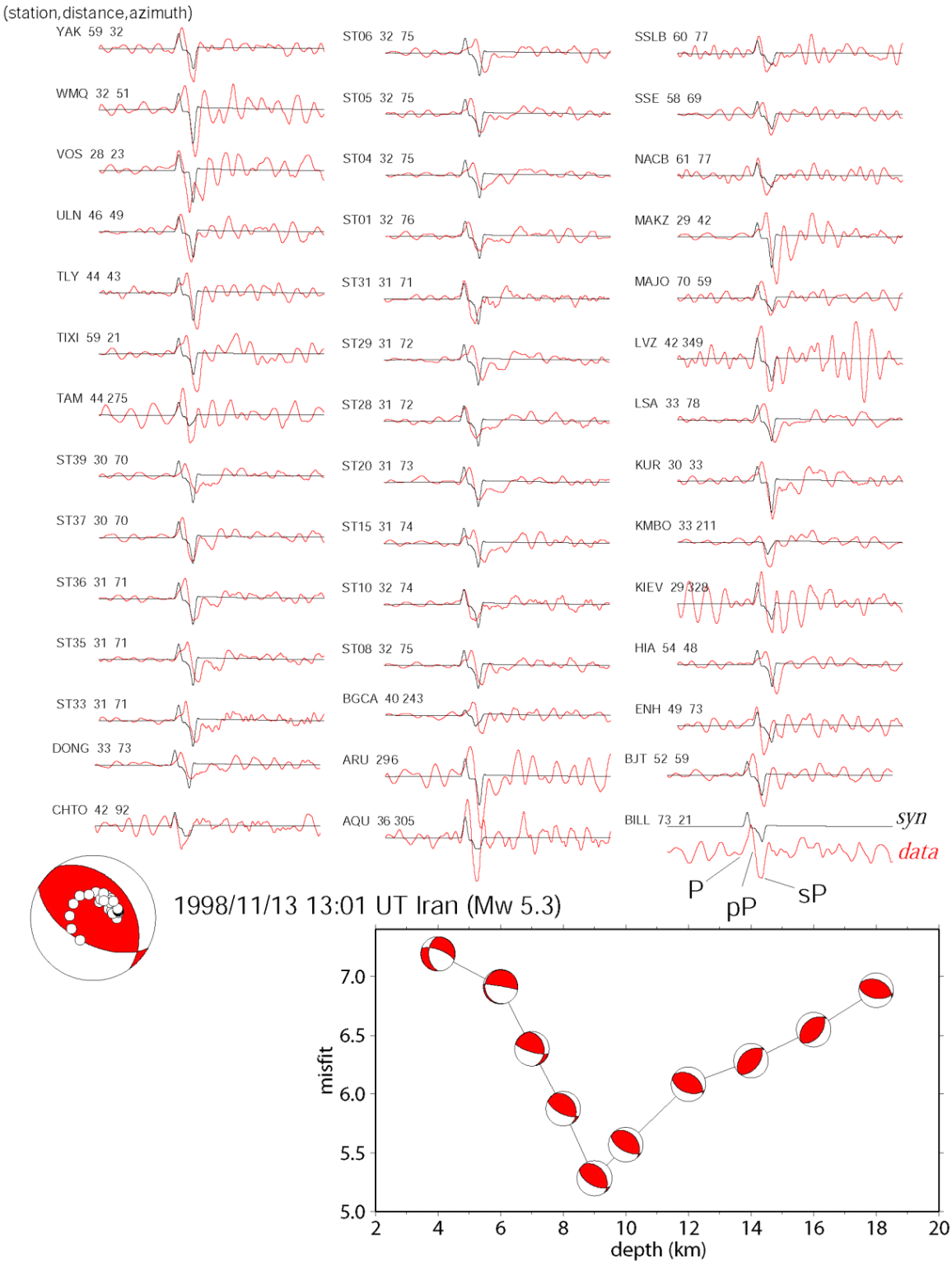

Figure 4. Focal Mechanism and hypocenter depth are estimated from the inversion of teleseismic P and depth phases using a grid search scheme. Note that the best depth for this event is 9 km.

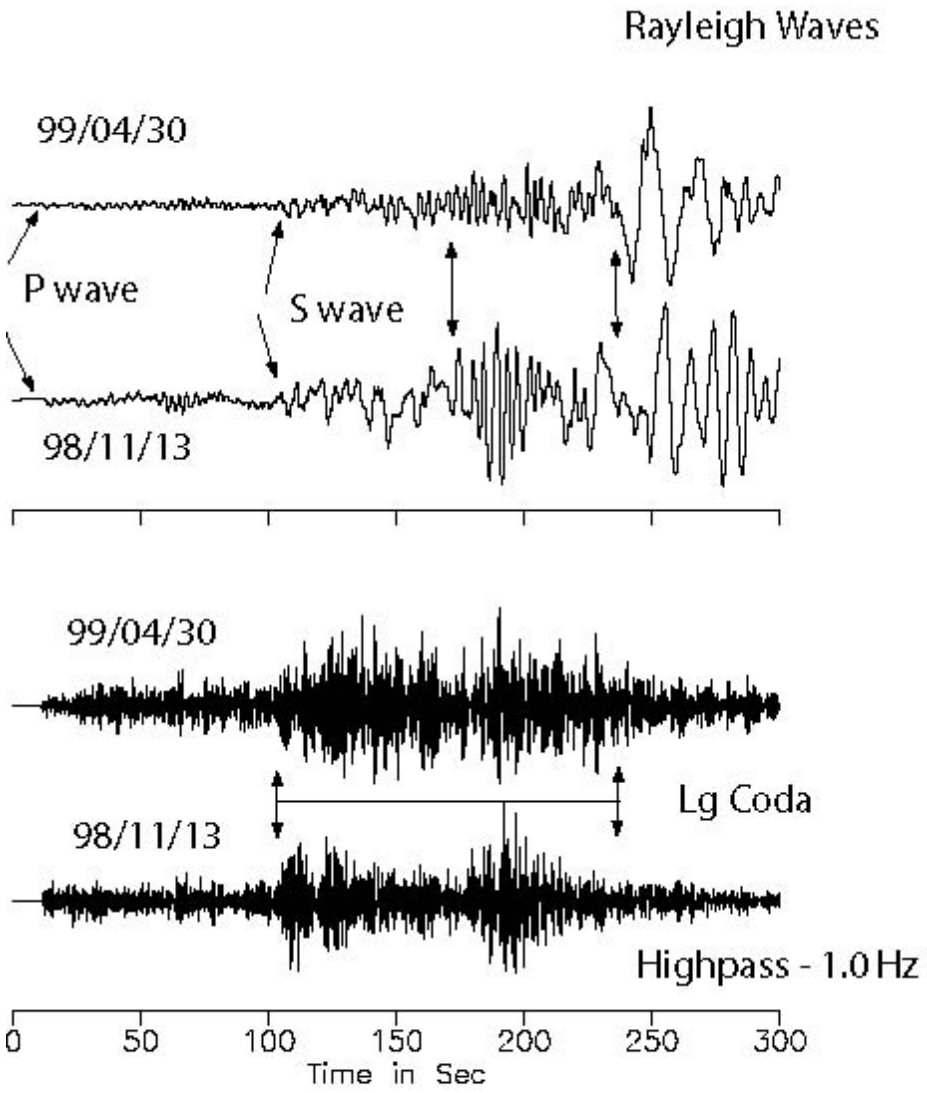

Figure 5. Comparison of seismograms recorded at RAYN (Saudi Arabia ~ 980 km) from the 04/30/99 earthquake with the seismograms recorded from the 11/13/98 (M_w 5.3) at two frequency bands. The top seismograms are the broadband displacements and the bottom seismograms are filtered versions at high frequency (>1Hz). Note the extension of Lg coda on the seismogram of 04/30/99 event suggesting that this earthquake must have occurred at shallow depth. The depth of the November event is about 9 km

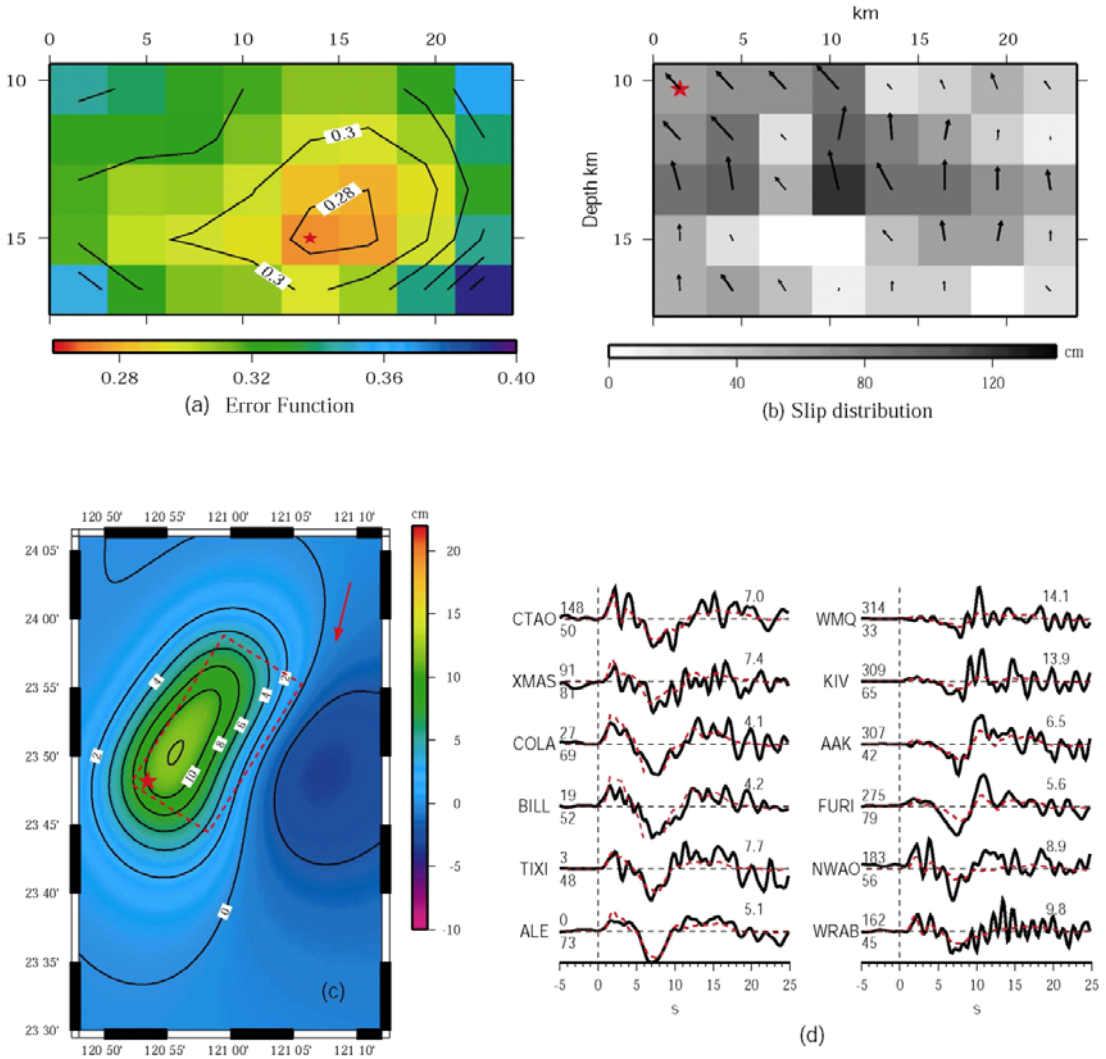

Figure 6. Determining hypocentral position by combined inverting teleseismic and Insar data. (a) Error function values when we put the hypocenter in the center of different subfaults. Star shows the target postion of hypocenter. (b) Inverted slip distribution when we put hypocenter at the upper-left corner. Star shows the position of hypocenter. Corresponding synthetics of InSar and seismic waves are shown in (c) and (d), respectively.